Nat. Hazards Earth Syst. Sci. Discuss.,
https://doi.org/10.5194/nhess-2020-41-AC6, 2020

Natural Hazards and Earth System Sciences
Discussions
Open Access
EGU

Interactive comment on "Comparison of machine learning classification algorithms for land cover change in a coastal area affected by the 2010 Earthquake and Tsunami in Chile" *by* Matias I. Volke and Rodrigo Abarca-Del-Rio

Matias I. Volke and Rodrigo Abarca-Del-Rio

matiasvolke@udec.cl

Received and published: 2 July 2020

The thematic maps for all the ML algorithms are presented in the appendix. The ML algorithms produced similar thematic maps, coherent in the classes and with a minimum of spots. By using McNemar's chi-squared ($\chi 2$) test we compared the significance of the differences between the results of the error matrices of the algorithms, showing p-values lower than 5624e-7, so there are no significant differences between the results shown by the different thematic maps (thematic maps in Figure 1 to 4). For these reasons, the analysis of land cover changes is performed based on the best performance

Printer-friendly version

Discussion paper

algorithm. In figure 5 and 6 are presented a tables with the results of Average overall accuracies and their coefficient of variation for ML algorithms applied in the 10 training subsamples. In figure 6 are summarized the Wilcoxon test results between different model to evaluate the significance of the differences in accuracy of the algorithms. In figure 7 a comparison between The highest average value obtained of overall accuracy for the ML classifiers is presented.

Interactive comment on Nat. Hazards Earth Syst. Sci. Discuss., https://doi.org/10.5194/nhess-2020-41, 2020.

Appendix B

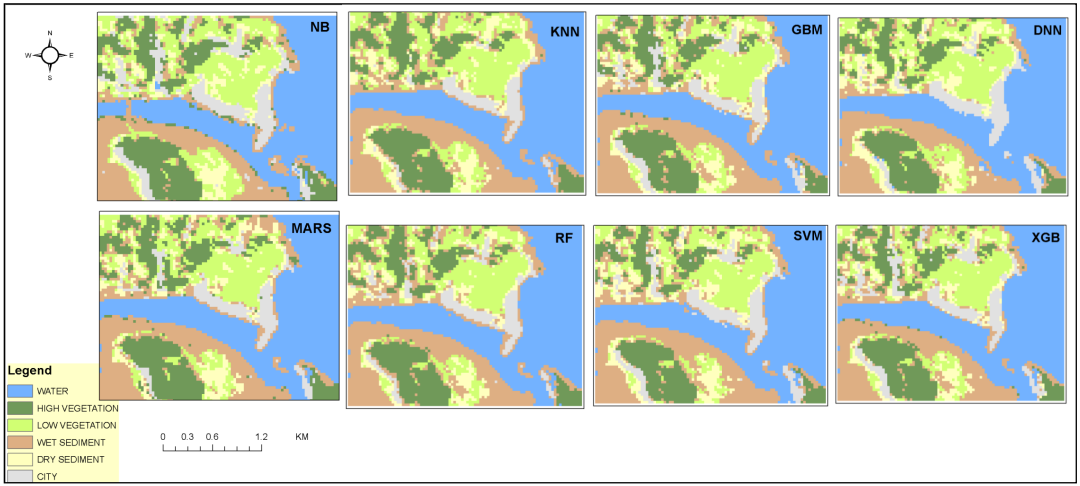

Fig B1. The thematic maps generated by the NB, KNN, GBM, DNN, MARS, RF, SVM, XGB classifications algorithms, focused on Tubul before 27-F. Thematic maps for Landsat image.

Fig. 1. . The thematic maps generated by the NB, KNN, GBM, DNN, MARS, RF, SVM, XGB classifications algorithms, focused on Tubul before 27-F. Thematic maps for Landsat image.

Printer-friendly version

Discussion paper

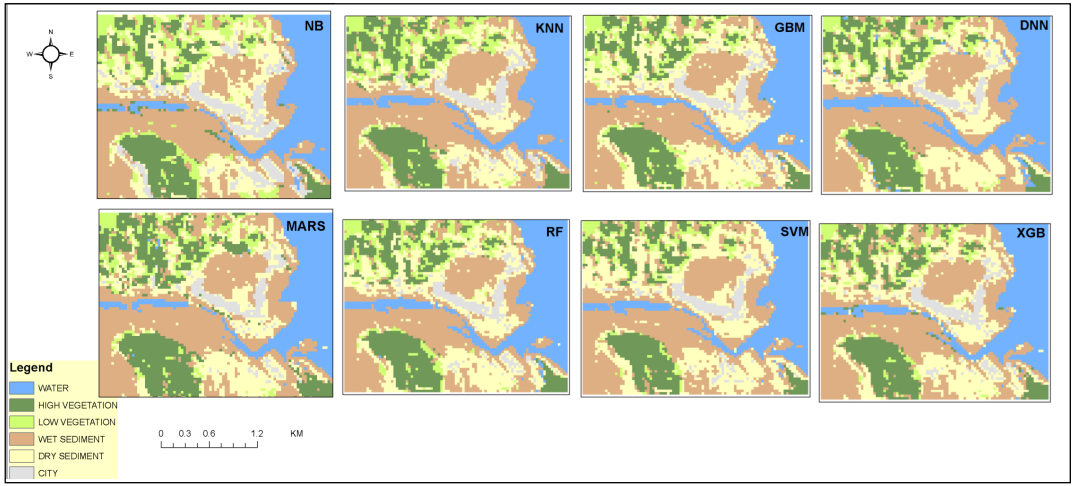

Fig B2. The thematic maps generated by the NB, KNN, GBM, DNN, MARS, RF, SVM, XGB classifications algorithms, focused on Tubul after 27-F. Thematic maps for Aster image.

Fig. 2. The thematic maps generated by the NB, KNN, GBM, DNN, MARS, RF, SVM, XGB classifications algorithms, focused on Tubul after 27-F. Thematic maps for Aster image.

Printer-friendly version

Discussion paper

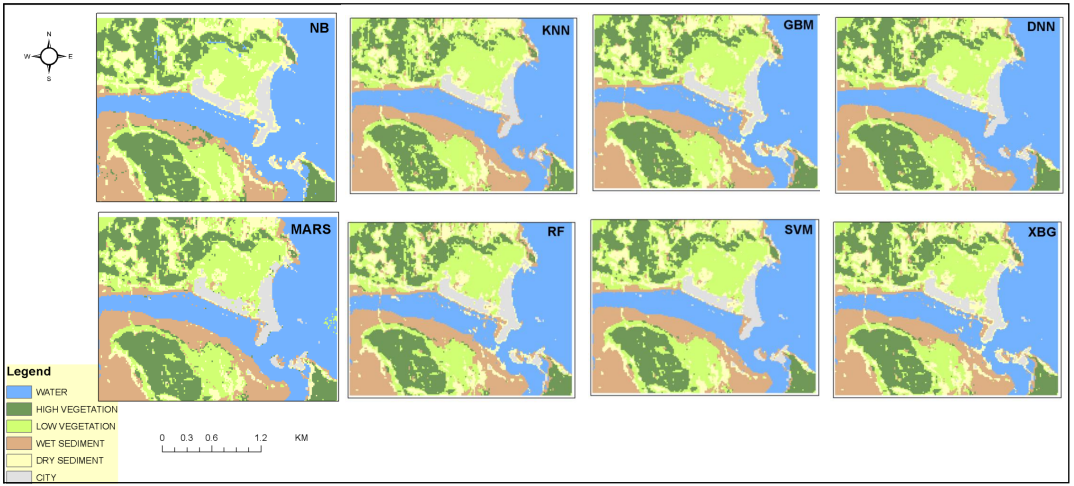

Fig B3. The thematic maps generated by the NB, KNN, GBM, DNN, MARS, RF, SVM, XGB classifications algorithms, focused on Tubul before 27-F. Thematic maps for Aster image.

Fig. 3. The thematic maps generated by the NB, KNN, GBM, DNN, MARS, RF, SVM, XGB classifications algorithms, focused on Tubul before 27-F. Thematic maps for Aster image.

Printer-friendly version

Discussion paper

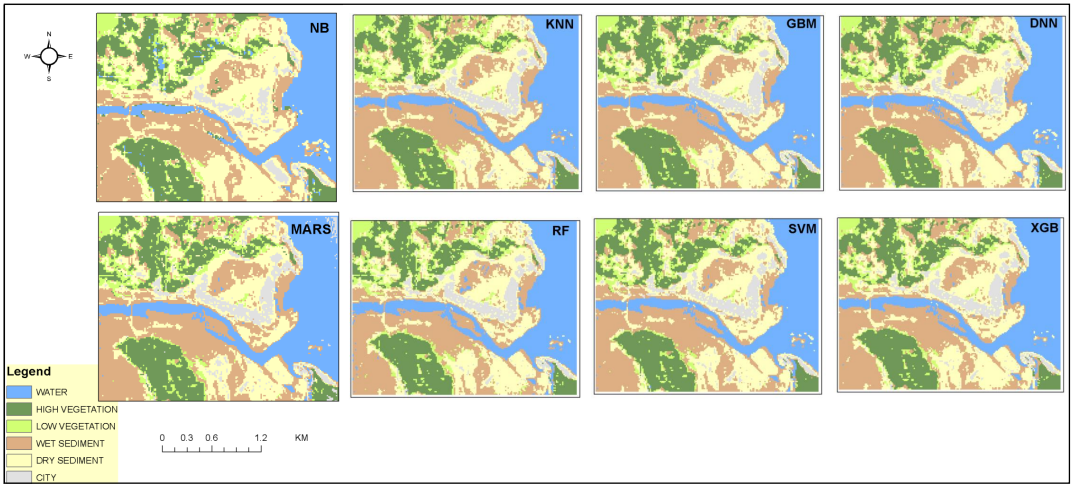

Fig B4. The thematic maps generated by the NB, KNN, GBM, DNN, MARS, RF, SVM, XGB classifications algorithms, focused on Tubul after 27-F. Thematic maps for Aster image.

Fig. 4. . The thematic maps generated by the NB, KNN, GBM, DNN, MARS, RF, SVM, XGB classifications algorithms, focused on Tubul after 27-F. Thematic maps for Aster image.

Printer-friendly version

Discussion paper

Landsat																				
Algorithm	**10%**		**20%**		**30%**		**40%**		**50%**		**60%**		**70%**		**80%**		**90%**		**100%**	
	mean	stde	mean	stde	mean	stde	mean	stde	mean	stde	mean	stde	mean	stde	mean	stde	mean	stde	mean	stde
NB	0.895	0.013	0.908	0.011	0.909	0.010	0.912	0.008	0.913	0.006	0.914	0.005	0.915	0.004	0.914	0.003	0.915	0.002	0.914	0.002
KNN	0.911	0.009	0.922	0.008	0.927	0.007	0.931	0.006	0.934	0.005	0.937	0.005	0.938	0.004	0.938	0.003	0.939	0.001	0.939	0.001
MARS	0.884	0.014	0.904	0.010	0.911	0.007	0.918	0.007	0.921	0.005	0.924	0.005	0.925	0.004	0.925	0.003	0.926	0.001	0.927	0.001
GBM	0.899	0.012	0.917	0.010	0.925	0.008	0.933	0.007	0.936	0.005	0.940	0.004	0.942	0.003	0.943	0.004	0.945	0.003	0.946	0.002
SVM	0.916	0.009	0.932	0.008	0.939	0.006	0.943	0.005	0.947	0.004	0.950	0.004	0.952	0.003	0.953	0.002	0.955	0.001	0.955	0.001
RF	0.917	0.010	0.927	0.007	0.933	0.006	0.936	0.006	0.939	0.005	0.940	0.005	0.941	0.004	0.943	0.004	0.943	0.003	0.942	0.002
DNN	0.925	0.011	0.939	0.009	0.934	0.009	0.934	0.008	0.938	0.008	0.945	0.007	0.946	0.005	0.948	0.004	0.949	0.001	0.949	0.001
XGB	0.904	0.016	0.920	0.012	0.927	0.010	0.933	0.007	0.939	0.006	0.942	0.005	0.946	0.004	0.947	0.003	0.951	0.001	0.952	0.001

Fig. 5. Average overall accuracies and their coefficient of variation for ML algorithms applied in all training sample size (Landsat images).

Aster																				
Algorithm	**10%**		**20%**		**30%**		**40%**		**50%**		**60%**		**70%**		**80%**		**90%**		**100%**	
	mean	stde	mean	stde	mean	stde	mean	stde	mean	stde	mean	stde	mean	stde	mean	stde	mean	stde	mean	stde
NB	0.924	0.013	0.923	0.007	0.931	0.007	0.934	0.011	0.932	0.007	0.933	0.005	0.933	0.005	0.932	0.002	0.934	0.001	0.934	0.001
KNN	0.925	0.014	0.940	0.010	0.954	0.006	0.957	0.005	0.964	0.004	0.966	0.002	0.967	0.003	0.970	0.002	0.971	0.002	0.971	0.002
MARS	0.942	0.010	0.952	0.021	0.949	0.011	0.959	0.022	0.959	0.021	0.967	0.004	0.967	0.007	0.969	0.014	0.969	0.002	0.970	0.002
GBM	0.935	0.010	0.958	0.008	0.965	0.004	0.968	0.004	0.970	0.002	0.973	0.003	0.974	0.002	0.975	0.002	0.975	0.001	0.975	0.001
SVM	0.944	0.012	0.962	0.008	0.967	0.005	0.971	0.006	0.975	0.003	0.976	0.004	0.976	0.003	0.977	0.001	0.979	0.001	0.979	0.001
RF	0.930	0.015	0.957	0.014	0.963	0.003	0.965	0.004	0.967	0.003	0.970	0.002	0.971	0.002	0.972	0.002	0.974	0.001	0.973	0.001
DNN	0.945	0.002	0.951	0.001	0.961	0.002	0.964	0.001	0.967	0.002	0.968	0.004	0.969	0.003	0.972	0.001	0.973	0.001	0.973	0.001
XGB	0.935	0.013	0.957	0.009	0.965	0.004	0.966	0.005	0.969	0.002	0.971	0.004	0.974	0.002	0.973	0.002	0.974	0.001	0.976	0.001

Fig. 6. Average overall accuracies and their coefficient of variation for ML algorithms applied in all training sample size (Aster images).

Landsat				Aster				Landsat-Aster	
No	p.value	No	p.value	No	p.value	No	p.value	No	p.value
NB vs. KNN	<0.001	MARS vs. SVM	<0.001	NB vs. KNN	<0.001	MARS vs. SVM	<0.001	NB	<0.001
NB vs. MARS	<0.001	MARS vs. RF	<0.001	NB vs. MARS	<0.001	MARS vs. RF	0.064	KNN	<0.001
NB vs. GBM	<0.001	MARS vs. DNN	0.084	NB vs. GBM	<0.001	MARS vs. DNN	0.004	MARS	<0.001
NB vs. SVM	<0.001	MARS vs. XGB	0.033	NB vs. SVM	<0.001	MARS vs. XGB	0.037	GBM	0.006
NB vs. RF	<0.001	GBM vs. SVM	<0.001	NB vs. RF	<0.001	GBM vs. SVM	<0.001	SVM	0.006
NB vs. DNN	<0.001	GBM vs. RF	<0.001	NB vs. DNN	<0.001	GBM vs. RF	<0.001	RF	<0.001
NB vs. XGB	<0.001	GBM vs. DNN	0.084	NB vs. XGB	<0.001	GBM vs. DNN	0.084	DNN	<0.001
KNN vs. MARS	0.906	GBM vs. XGB	0.033	KNN vs. MARS	0.906	GBM vs. XGB	0.033	XGB	<0.001
KNN vs. GBM	<0.001	SVM vs RF	0.006	KNN vs. GBM	<0.001	SVM vs RF	0.006		
KNN vs. SVM	<0.001	SVM vs DNN	0.004	KNN vs. SVM	<0.001	SVM vs DNN	0.004		
KNN vs. RF	<0.001	SVM vs XGB	0.006	KNN vs. RF	<0.001	SVM vs XGB	0.006		
KNN vs. DNN	0.006	RF vs XGB	0.232	KNN vs. DNN	0.006	RF vs XGB	0.023		
KNN vs. XGB	<0.001	RF vs DNN	0.020	KNN vs. XGB	<0.001	RF vs DNN	0.088		
MARS vs. GBM	0.041	DNN vs XGB	0.084	MARS vs. GBM	0.041	DNN vs XGB	0.084		

Fig. 7. Table 6. Wilcoxon test results between different models for each image type and between images (significance achieved at $p < 0.05$)

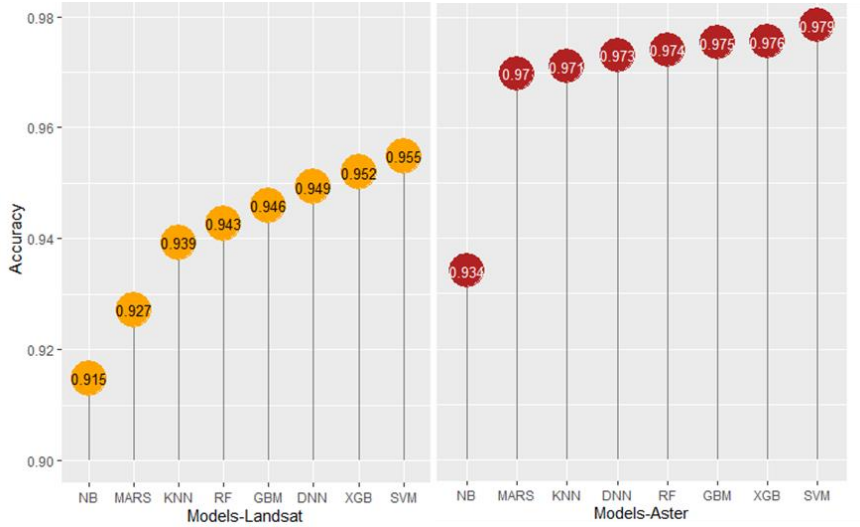

Fig. 8. The highest average value obtained from OA among the different sizes of training subsamples for the ML classifiers. For Landsat (left) and ASTER (right) images.

Printer-friendly version

Discussion paper